Joint Calibration and Tomography based on Separable Least Squares Approach with Constraints on Linear and Non-Linear Parameters

Venkata PATHURI-BHUVANA
Silicon Austria Labs
Linz, Austria
venkata.pathuri-bhuvana@silicon-austria.com

Stefan SCHUSTER
voestalpine Stahl GmbH, Austria
Linz, Austria
stefan.schuster2@voestalpine.com

Andreas OCH
Infineon Technologies Austria AG, Austria
Linz, Austria
Andreas.Och@infineon.com

***Abstract*—Most of the existing tomography techniques rely on accurate calibration to reconstruct the features of interest. In several industrial applications, the calibration is typically performed off-line and has to be repeated frequently to counter time varying perturbation caused by aging, operating conditions, and so on. In this paper, a novel online joint calibration and tomography method based on variable projection based separable least squares approach with constraints on linear and non-linear parameters is proposed. The constraints on the linear parameters improve the estimation accuracy of the ill-posed and under determined tomography problem. The constraints on the non-linear parameters restricts the proposed method from departing far away from the initial guess, especially when a good initial guess is available. The proposed method is used to reconstruct the temperature distribution inside a blast furnace and simultaneously to calibrate the positions of acoustic transducers based on simulated acoustic time of flight measurements.**

***Index Terms*—Tomography, online sensor calibration, constrained optimization.**

I. Introduction

Tomography is a well established technique of reconstructing certain features, usually in a 2D or 3D region of interest (RoI) from projections passing through it [1], [2]. In general, these projections are line of sight (LoS) paths from transducers such as radar, ultrasound, acoustic and so on that penetrate through the RoI [3], [4], [5]. A typical tomography problem can be modeled as inverse problem and techniques based on least squares and regularized least squares can be used to estimate the parameters related to the features of interest [6].

However, one of the key requirements of these algorithms is to have accurate information about the calibration parameters such as transducer positions to minimize the difference between ideal system model and real world measurements [3], [5]. In order to accurately estimate the calibration parameters, typically, the RoI is filled with known features and then calibration is performed by associating the corresponding measurements with the known features [3], [7], [8]. Though this approach yields accurate results, the calibration process needs to be repeated frequently to counter the unwanted and time varying perturbation due to aging, operating conditions and so on. The practical limitations of repeatedly replacing the RoI features with known features can make this calibration approach expensive and cumbersome. To avoid this problem, authors in [9] have proposed online self-calibration approach in which the same set of measurements is used to estimate both the calibration and tomography parameters. This approach essentially models the problem as a least squares problem and performs alternating minimization with respect to the calibration and tomography parameters. The alternating minimization often converges very slowly. The coupled optimization of calibration and tomography parameters can improve the least squares optimization efficiency [10] and results in an online joint calibration and tomography (JCT) method.

In this paper, the JCT method based on a separable least squares (SLS) approach is proposed. The proposed method models the tomography and calibration parameters in the system model as linear and non-linear parameters, respectively. The variable projection (VP) approach is used to solve the coupled optimization in the form of SLS [11]. Further, this paper uses constraints on the linear and non-linear parameters. The constraints on the linear (tomographic) parameters improves the estimation accuracy when the given problem is ill-posed and under determined such as the JCT. The goal of imposing constraints on the non-linear (calibration) parameters is to restrict the optimization algorithm from departing far away from the initial guess of the calibration parameters. Thus, the proposed algorithm can efficiently find the global minimum when a good initial guess is available as in the case of JCT. In [10], [12], authors presented the VP method with constraints on linear parameters. This paper further adapts the VP method such that constraints can be imposed on non-linear parameters. In addition, this paper provides the approximated solutions for computing the Jacobian matrix and gradient vector which are required for solving the non-linear optimization problem. The approximated Jacobian matrix and gradient vector can significantly decrease the number of function evaluations and iterations required to converge to the global minimum compared to the finite difference methods used by non-linear optimization methods provided by Matlab. Further, simulated acoustic time of flight (ToF) measurements are used to evaluate the proposed JCT method for reconstructing the temperature distribution inside a blast furnace and calibrate the acoustic

transducer positions.

The paper is organized as follows: Sec. II describes the acoustic system model. Sec. III introduces the basics of the VP based SLS method. Sec. IV describes the proposed VP based JCT with constraints on linear and non-linear parameters. Sec. V evaluates the proposed method based on simulated data. Sec. VI presents the conclusions.

II. System Model

Let us consider a 2D circular RoI as shown in the Fig. 1, which is divided into uniform mesh grid cells. In order to observe the features within the RoI, a set of N_s transducers that can transmit and receive signals such as radar, ultrasound, x-rays, and so on are placed around its circumference. Without loosing generality of the tomography problem, this paper evaluates the proposed methods using the ToF tomography with acoustic signals to reconstruct the temperature distribution inside the RoI. Thus, the following system model corresponds to the acoustic ToF tomography for a blast furnace application. For more details, readers are referred to [13]. However, it can be generalized to a wide range of tomography problems with different transducers and materials in the RoI.

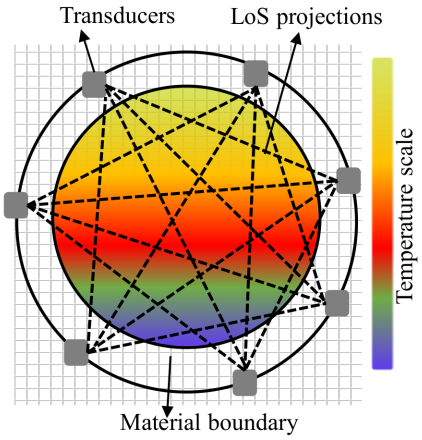

Fig. 1: An illustration of 2D time of flight tomography.

Let us consider τ_{ij} is the ToF of the acoustic signal between transducers i and j, where $i, j = 1, 2, 3...N_s$ and $i \neq j$ and it is given as

$$\tau_{ij} = \sum_{k=1}^{N_\mathrm{g}} h_{ij}^{k}\left(\alpha_{ij}\right) s^{k} + v_{ij} = \sum_{k=1}^{N_\mathrm{g}} d_{ij}^{k} s^{k} + v_{ij}, \qquad (1)$$

where

- N_g is the number of the unit grid cells.
- $h_{ij}^{k}\left(\alpha_{ij}\right) = d_{ij}^{k}$, where d_{ij}^{k} is the distance traveled by the acoustic signal in the unit grid cell k as a function of transducer positions $\alpha_{ij} = \left[x_i, x_j, y_i, y_j\right]^T$.
- $s^{k} \propto 1/\sqrt{T^{k}}$ is the slowness parameter (linear tomography parameter) as a function of the temperature T^{k} in the grid cell k.
- v_{ij} is independent and identically (IID) distributed measurement noise.

The ToF measurements of all the acoustic LoS paths between the possible transducer combinations can be written in the matrix form as

$$\boldsymbol{\tau} = \left[\mathbf{h}^{1}\left(\boldsymbol{\alpha}\right)\mathbf{h}^{2}\left(\boldsymbol{\alpha}\right)\cdots\mathbf{h}^{N_g}\left(\boldsymbol{\alpha}\right)\right]\mathbf{s} + \mathbf{v} = \mathbf{H}\left(\boldsymbol{\alpha}\right)\mathbf{s} + \mathbf{v}, \qquad (2)$$

where

- $\boldsymbol{\tau}$ is measurement vector of length $N_\mathrm{p} \times 1$ where N_p is the number LoS paths.
- $\boldsymbol{\alpha} = \left[x_1, x_2, \cdots x_{N_s}, y_1, y_2, \cdots, y_{N_s}\right]^T$ is a vector of length $2N_s \times 1$ containing the transducer positions.
- $\mathbf{h}^{k}\left(\boldsymbol{\alpha}\right)$ is column vector containing values of $h_{ij}^{k}\left(\alpha_{ij}\right)$ $\forall \quad i, j = 1, 2, 3...N_s \wedge i \neq j$.
- $\mathbf{H}\left(\boldsymbol{\alpha}\right)$ is a $N_\mathrm{p} \times N_\mathrm{g}$ measurement matrix as a function of transducer positions $\boldsymbol{\alpha}$.
- $\mathbf{s}$ is the slowness vector of length $N_\mathrm{g} \times 1$.
- $\mathbf{v}$ is the IID measurement noise vector of length $N_\mathrm{p} \times 1$.

The goal of this paper is to estimate the slowness vector $\mathbf{s}$ and transducer positions $\boldsymbol{\alpha}$ given the ToF measurement vector $\boldsymbol{\tau}$. Once the estimated slowness vector $\hat{\mathbf{s}}$ is known, the temperature distribution within the ROI can be estimated as $1/\hat{\mathbf{s}}^2$. The following section briefly explains the VP based SLS methodology which forms the basis for the proposed method.

III. Variable Projection based Separable Least Squares

Given the data $\boldsymbol{\tau}$, the VP method estimates the parameters $\mathbf{s}$ and $\boldsymbol{\alpha}$ by minimizing the following least squares cost function

$$r\left(\mathbf{s}, \boldsymbol{\alpha}\right) = \left\|\boldsymbol{\tau} - \mathbf{H}\left(\boldsymbol{\alpha}\right)\mathbf{s}\right\|_2^2 \qquad (3)$$

with respect to $\mathbf{s}$ and $\boldsymbol{\alpha}$. However, the cost function $r\left(\mathbf{s}, \boldsymbol{\alpha}\right)$ falls into a special category where the parameters to be estimated can be separated into linear and non-linear parameters, i.e., $\mathbf{s}$ being the linear and $\boldsymbol{\alpha}$ being the non-linear parameters. In order to explore this separation, a modified cost function is written as

$$r_1\left(\boldsymbol{\alpha}\right) = \left\|\boldsymbol{\tau} - \mathbf{H}\left(\boldsymbol{\alpha}\right)\mathbf{H}^{+}\left(\boldsymbol{\alpha}\right)\boldsymbol{\tau}\right\|_2^2 = \left\|\mathbf{P}^{\perp}\left(\boldsymbol{\alpha}\right)\boldsymbol{\tau}\right\|_2^2, \qquad (4)$$

where $\mathbf{H}^{+}\left(\boldsymbol{\alpha}\right) = \left(\mathbf{H}^{T}\left(\boldsymbol{\alpha}\right)\mathbf{H}\left(\boldsymbol{\alpha}\right)\right)^{-1}\mathbf{H}^{T}\left(\boldsymbol{\alpha}\right)$ is the pseudo inverse of the observation matrix $\mathbf{H}\left(\boldsymbol{\alpha}\right)$ and $\mathbf{P}^{\perp}\left(\boldsymbol{\alpha}\right)$ is the complement orthogonal projection matrix. Once the optimal estimate $\hat{\boldsymbol{\alpha}}$ is determined by minimizing the above cost function with respect to $\boldsymbol{\alpha}$, the optimal estimate of the linear parameter $\mathbf{s}$ can be determined as

$$\hat{\mathbf{s}} = \mathbf{H}^{+}\left(\hat{\boldsymbol{\alpha}}\right)\boldsymbol{\tau}. \qquad (5)$$

In [11], the authors have proved that if the $\hat{\boldsymbol{\alpha}}$ is a global minimizer of $r_1\left(\boldsymbol{\alpha}\right)$ then the set of corresponding $\hat{\mathbf{s}}$ as given in (5) and $\hat{\boldsymbol{\alpha}}$ is a global minimizer of $r\left(\mathbf{s}, \boldsymbol{\alpha}\right)$ and $r\left(\hat{\mathbf{s}}, \hat{\boldsymbol{\alpha}}\right) = r_1\left(\hat{\boldsymbol{\alpha}}\right)$. Several non-linear solvers based on Gauss-Newton, Levenberg-Marquardt algorithms can be used to minimize the cost function $r_1\left(\boldsymbol{\alpha}\right)$. Authors in [11] further provided the approximated solutions for computing the Jacobian matrix $\mathbf{J}_{r_1}$ and the gradient $\boldsymbol{\nabla}_{r_1}$ which improve the efficiency of the mentioned non-linear solvers by reducing the number of iterations required to converge to the global minimum. Further

details on how to compute the Jacobian matrix and the gradient are provided in the next section.

IV. The JCT based on VP Method with Constraints on Linear and Non-Linear Parameters

Since the number of measurements N_p is considered to be far less than the number of linear parameters N_g and due to discretization, the tomographic reconstruction (estimation of the linear parameters) becomes an ill-posed and under determined problem. Thus, adding a regularization term on the linear parameters $\mathbf{s}$ to the cost function $r(\mathbf{s}, \boldsymbol{\alpha})$ can address this problem by smoothing the RoI. Furthermore, since a good initial guess $\boldsymbol{\alpha}_0$ of the calibration parameters is provided, adding a constraint on $(\boldsymbol{\alpha} - \boldsymbol{\alpha}_0)$ can enforce the optimization to find the minimum around the initial guess. With these considerations, a modified cost function can be defined as

$$\begin{aligned} r_2(\mathbf{s}, \boldsymbol{\alpha}) &= \|\boldsymbol{\tau} - \mathbf{H}(\boldsymbol{\alpha})\mathbf{s}\|_2^2 + \|\boldsymbol{\Lambda}\mathbf{s}\|_2^2 + \|\boldsymbol{\Gamma}(\boldsymbol{\alpha} - \boldsymbol{\alpha}_0)\|_2^2, \\ &= \left\| \begin{bmatrix} \boldsymbol{\tau} \\ \mathbf{0} \end{bmatrix} - \begin{bmatrix} \mathbf{H}(\boldsymbol{\alpha}) \\ \boldsymbol{\Lambda} \end{bmatrix} \mathbf{s} \right\|_2^2 + \|\boldsymbol{\Gamma}(\boldsymbol{\alpha} - \boldsymbol{\alpha}_0)\|_2^2, \\ &= \left\| \begin{bmatrix} \boldsymbol{\tau} \\ \mathbf{0} \end{bmatrix} - \mathbf{H}_{\boldsymbol{\Lambda}}(\boldsymbol{\alpha})\mathbf{s} \right\|_2^2 + \|\boldsymbol{\Gamma}(\boldsymbol{\alpha} - \boldsymbol{\alpha}_0)\|_2^2, \end{aligned} \tag{6}$$

where $\boldsymbol{\Lambda}$ is a $N_\mathrm{g} \times N_\mathrm{g}$ regularization matrix, $\boldsymbol{\Gamma}$ is a $2N_\mathrm{s} \times 2N_\mathrm{s}$ penalty matrix and $\mathbf{H}_{\boldsymbol{\Lambda}}(\boldsymbol{\alpha}) = [\mathbf{H}(\boldsymbol{\alpha})\ \boldsymbol{\Lambda}]^T$. The variable separation is achieved by writing the linear parameters $\mathbf{s}$ in (6) as a function of non-linear parameters $\boldsymbol{\alpha}$. Thus, the modified cost function is written as

$$\begin{aligned} r_3(\boldsymbol{\alpha}) &= \|\mathbf{f}(\boldsymbol{\alpha})\|_2^2, \\ &= \left\| \begin{bmatrix} \boldsymbol{\tau} \\ \mathbf{0} \end{bmatrix} - \mathbf{H}_{\boldsymbol{\Lambda}}(\boldsymbol{\alpha})\mathbf{H}_{\boldsymbol{\Lambda}}^+(\boldsymbol{\alpha}) \begin{bmatrix} \boldsymbol{\tau} \\ \mathbf{0} \end{bmatrix} \right\|_2^2 + \|\boldsymbol{\Gamma}(\boldsymbol{\alpha} - \boldsymbol{\alpha}_0)\|_2^2, \\ &= \left\| \left[\mathbf{I} - \mathbf{H}_{\boldsymbol{\Lambda}}(\boldsymbol{\alpha})\mathbf{H}_{\boldsymbol{\Lambda}}^+(\boldsymbol{\alpha})\right] \begin{bmatrix} \boldsymbol{\tau} \\ \mathbf{0} \end{bmatrix} \right\|_2^2 + \|\boldsymbol{\Gamma}(\boldsymbol{\alpha} - \boldsymbol{\alpha}_0)\|_2^2, \\ &= \left\| \mathbf{P}_{\boldsymbol{\Lambda}}^{\perp}(\boldsymbol{\alpha}) \begin{bmatrix} \boldsymbol{\tau} \\ \mathbf{0} \end{bmatrix} \right\|_2^2 + \|\boldsymbol{\Gamma}(\boldsymbol{\alpha} - \boldsymbol{\alpha}_0)\|_2^2, \end{aligned} \tag{7}$$

where $\mathbf{H}_{\boldsymbol{\Lambda}}^+(\boldsymbol{\alpha})$ is the pseudo inverse matrix which is given as

$$\mathbf{H}_{\boldsymbol{\Lambda}}^+(\boldsymbol{\alpha}) = \left(\mathbf{H}_{\boldsymbol{\Lambda}}^T(\boldsymbol{\alpha})\mathbf{H}_{\boldsymbol{\Lambda}}(\boldsymbol{\alpha})\right)^{-1}\mathbf{H}_{\boldsymbol{\Lambda}}^T(\boldsymbol{\alpha}), \tag{8}$$

$\mathbf{P}_{\boldsymbol{\Lambda}}^{\perp}(\boldsymbol{\alpha}) = \left[\mathbf{I} - \mathbf{H}_{\boldsymbol{\Lambda}}(\boldsymbol{\alpha})\mathbf{H}_{\boldsymbol{\Lambda}}^+(\boldsymbol{\alpha})\right]$ is the orthogonal complement matrix and $\mathbf{I}$ is the identity matrix. The estimate $\hat{\boldsymbol{\alpha}}$ can be determined by minimizing the cost function in (7) as

$$\hat{\boldsymbol{\alpha}} = \arg\min_{\boldsymbol{\alpha}} r_3(\boldsymbol{\alpha}). \tag{9}$$

Once the optimal estimate $\hat{\boldsymbol{\alpha}}$ of the non-linear parameter is determined, the estimate of the linear parameter $\mathbf{s}$ can be determined as

$$\hat{\mathbf{s}} = \mathbf{H}_{\boldsymbol{\Lambda}}^+(\hat{\boldsymbol{\alpha}}) \begin{bmatrix} \boldsymbol{\tau} \\ \mathbf{0} \end{bmatrix}. \tag{10}$$

Several non-linear solvers based on Gauss-Newton and Levenberg-Marquardt algorithms can be used to minimize the residual $r_3(\boldsymbol{\alpha})$. However, in order to implement these algorithms, evaluation of the gradient vector and Jacobian matrix are required. In order to calculate them, let us rewrite the cost function in (7) as

$$r_3(\boldsymbol{\alpha}) = \|\mathbf{f}(\boldsymbol{\alpha})\|_2^2 = \left\| \begin{bmatrix} \mathbf{P}_{\boldsymbol{\Lambda}}^{\perp}(\boldsymbol{\alpha}) \begin{bmatrix} \boldsymbol{\tau} \\ \mathbf{0} \end{bmatrix} \\ \boldsymbol{\Gamma}(\boldsymbol{\alpha} - \boldsymbol{\alpha}_0) \end{bmatrix} \right\|_2^2. \tag{11}$$

The Jacobian of $\mathbf{f}(\boldsymbol{\alpha})$ can be written as

$$\mathbf{J}_{\mathbf{f}(\boldsymbol{\alpha})} = \begin{bmatrix} \mathbf{J}_{\mathbf{H}_{\boldsymbol{\Lambda}}^+(\boldsymbol{\alpha})} \\ \boldsymbol{\Gamma} \end{bmatrix}, \tag{12}$$

where $\mathbf{J}_{\mathbf{H}_{\boldsymbol{\Lambda}}^+(\boldsymbol{\alpha})}$ is the Jacobian of the $\mathbf{H}_{\boldsymbol{\Lambda}}^+(\boldsymbol{\alpha})$. For simplicity, we omit the non-linear parameters $\boldsymbol{\alpha}$ in the following. From [11], the k-th column of the $\mathbf{J}_{\mathbf{H}_{\boldsymbol{\Lambda}}^+}$ is given as

$$\left[\mathbf{J}_{\mathbf{H}_{\boldsymbol{\Lambda}}^+}\right]_k = -\left(\mathbf{P}_{\boldsymbol{\Lambda}}\mathbf{D}_k\mathbf{H}_{\boldsymbol{\Lambda}}^+ + \left(\mathbf{P}_{\boldsymbol{\Lambda}}\mathbf{D}_k\mathbf{H}_{\boldsymbol{\Lambda}}^+\right)^T\right) \begin{bmatrix} \boldsymbol{\tau} \\ \mathbf{0} \end{bmatrix}, \tag{13}$$

where $\mathbf{P}_{\boldsymbol{\Lambda}} = \mathbf{H}_{\boldsymbol{\Lambda}}\mathbf{H}_{\boldsymbol{\Lambda}}^+$ is the projection matrix and $\mathbf{D}_k = \partial\mathbf{H}_{\boldsymbol{\Lambda}}(\boldsymbol{\alpha})/\partial\alpha_k$ represents the matrix of partial derivatives of $\mathbf{H}_{\boldsymbol{\Lambda}}(\boldsymbol{\alpha})$ with respect to the single parameter α_k. Now, the gradient of the functional $\mathbf{f}(\boldsymbol{\alpha})$ can be computed as

$$\boldsymbol{\nabla}_{\mathbf{f}(\boldsymbol{\alpha})} = 2\mathbf{J}_{\mathbf{f}(\boldsymbol{\alpha})}^T\mathbf{f}(\boldsymbol{\alpha}) = 2\mathbf{J}_{\mathbf{f}(\boldsymbol{\alpha})}^T \begin{bmatrix} \mathbf{P}_{\boldsymbol{\Lambda}}^{\perp}(\boldsymbol{\alpha}) \begin{bmatrix} \mathbf{0} \\ \boldsymbol{\tau} \end{bmatrix} \\ \boldsymbol{\Gamma}(\boldsymbol{\alpha} - \boldsymbol{\alpha}_0) \end{bmatrix}. \tag{14}$$

Algorithm 1 illustrates the essential steps of the proposed method using the Gauss-Newton method.

Algorithm 1 The proposed JCT method based on VP approach with constraints on the linear and non-linear parameters.

- Choose initial $\hat{\boldsymbol{\alpha}}_0$
- **Recursion:** *For* $l = 0, 1, 2, 3, \cdots$
  1) Calculate $\mathbf{f}(\hat{\boldsymbol{\alpha}}_l)$ as shown in (11)
  2) Compute the Jacobian $\mathbf{J}_{\mathbf{H}_{\boldsymbol{\Lambda}}^+(\hat{\boldsymbol{\alpha}}_l)}^l$ as shown in (12)
  3) Compute the gradient $\boldsymbol{\nabla}_{\mathbf{f}(\hat{\boldsymbol{\alpha}}_l)}^l$ as shown in (14)
  4) Update the non-linear variable as

$$\hat{\boldsymbol{\alpha}}_{l+1} = \hat{\boldsymbol{\alpha}}_l - \left(\mathbf{J}_{\mathbf{H}_{\boldsymbol{\Lambda}}^+(\hat{\boldsymbol{\alpha}}_l)}^{l^T}\mathbf{J}_{\mathbf{H}_{\boldsymbol{\Lambda}}^+(\hat{\boldsymbol{\alpha}}_l)}^l\right)^{-1}\boldsymbol{\nabla}_{\mathbf{f}(\hat{\boldsymbol{\alpha}}_l)}^l \tag{15}$$

  end
- Calculate the linear variable $\hat{\mathbf{s}}_{l+1} = \mathbf{H}^+(\hat{\boldsymbol{\alpha}}_{l+1})\boldsymbol{\tau}$

V. Simulation Results

In this section, the proposed JCT method with constraints on the linear and non-linear parameters is compared with the method without constraints on the non-linear parameters. Both of these methods use VP based SLS approach. This simulation considers a circular RoI with $8.4\,\mathrm{m}$ diameter [13]. A set of 10 acoustic transducers is uniformly distributed on the circumference of a circular ring with $10\,\mathrm{m}$ diameter as shown in Fig. 2. Further, the RoI is divided into an uniform mesh grid of size $0.3\,\mathrm{m}$ by $0.3\,\mathrm{m}$. Each acoustic transducer can receive LoS projections from all other remaining transducers. In this setup, 97% of the grid cells in the RoI have at least one or more LoS paths passing through them as shown in

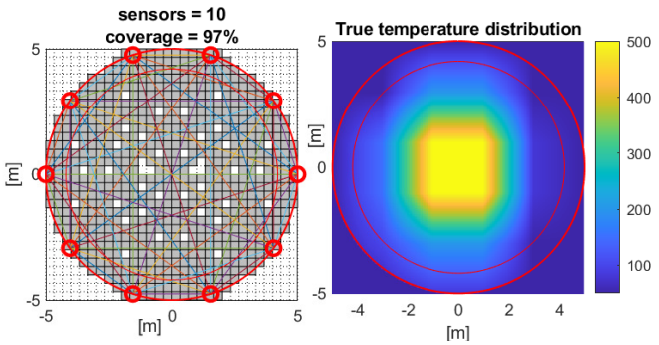

Fig. 2: Simulation setup in terms of the transducer positions and the ground truth temperature distribution inside the RoI.

Fig. 2. In Fig. 2, the grid cells with no LoS paths passing through them are depicted with white color. This figure also illustrates the simulated temperature distribution inside the RoI. With known positions of the transducers and temperature distribution, the ToF measurements can be obtained as shown in (2). The measurement noise vector $\mathbf{v}$ is simulated as zero mean IID Gaussian noise with variance $1e^{-6}$ which results in approximately $25\,\text{dB}$ of signal to noise ratio.

Fig. 3 illustrates the reconstructed temperature using the JCT method with constraints only on the linear parameters and the method with constraints on the linear and non-linear parameters. For this simulation, the linear regularization matrix is chosen as

$$\mathbf{\Lambda} = 2e^{-4}\begin{bmatrix} 2 & -1 & 0 & 0 & \cdots & 0 \\ -1 & 3 & -1 & 0 & \cdots & 0 \\ 0 & -1 & 3 & -1 & \cdots & 0 \\ \vdots & \ddots & \ddots & \ddots & \cdots & \vdots \\ 0 & 0 & 0 & \cdots & -1 & 2 \end{bmatrix} \tag{16}$$

and the constraints $\mathbf{\Gamma}$ on the non-linear parameter as a diagonal matrix with each diagonal element is equal to $1e^{-4}$. These values are chosen by using trial and error approach. An IID noise with zero mean and variance $4e^{-4}$m is added to the true transducer positions to obtain the initial guess $\boldsymbol{\alpha}_0$. From Fig 3a and Fig 3b, it can be observed that employing constraints on the non-linear parameters in addition to the constraints on the linear parameters improves the accuracy of tomographic reconstruction. The resolution of the reconstructed temperature distribution can be improved by increasing the number of transducers. However, this results in high computational effort due to the increase in the number of linear and non-linear parameters. The root mean square error (RMSE) between the true temperature and the estimated temperature of the proposed JCT method with constraints on the linear and the non-linear parameters and the method with constraints only on the linear parameters are $3.94\,^{\circ}\text{C}$ and $4.59\,^{\circ}\text{C}$, respectively, as shown in Fig. 3c. Thus, employing constraints on non-linear parameters reduces the RMSE by $14\,\%$. Since the same linear constraints $\mathbf{\Lambda}$ are used for both the methods, the improvement in tomographic reconstruction of JCT method with constraints on the linear and non-linear parameters originates from the accurate calibration of transducer positions.

Fig. 4 illustrates the estimated positions of the transducers using JCT method method with constraints on the linear and non-linear parameters and the method with constraints only on the linear parameters. The corresponding RMSE between the estimated $\hat{\boldsymbol{\alpha}}$ and the true $\boldsymbol{\alpha}$ non-linear parameters are $1.845\,\text{cm}$ and $2.434\,\text{cm}$, respectively. From this figure, it can be observed that imposing constraints on the non-linear parameters improves the accuracy of calibration in terms of the transducer positions. Under the assumed simulation conditions, the JCT method without constraints on the non-linear parameters can often get struck in a local minimum away from either initial guess or true value. Imposing constraints on the non-linear parameters helps the proposed algorithm by restricting the search space around the initial guess which helps in finding the global minimum efficiently, especially when a good initial guess is provided.

Finally, the computational efficiency of the proposed method is compared with the 'lsqnonlin' routine from the Matlab optimization tool box. The 'lsqnonlin' is a Matlab implementation of trust region reflective optimization routine and it can estimate the non-linear parameter $\boldsymbol{\alpha}$ by minimizing the residual function $\mathbf{f}(\boldsymbol{\alpha})$ given in (11). The 'lsqnonlin' routine can also implicitly compute the Jacobian $\mathbf{J}^{l}_{\mathbf{H}^{+}_{\mathbf{\Lambda}}(\boldsymbol{\alpha})}$ and the gradient $\boldsymbol{\nabla}^{l}_{\mathbf{f}(\boldsymbol{\alpha})}$ using a finite differences approach. For this comparison, the proposed method computes the Jacobian and gradient as given in (12) and (14), receptively, where as the 'lsqnonlin' routine uses the finite differences approach. The number of functional evaluations of the residual $\mathbf{f}(\boldsymbol{\alpha})$ required for the proposed method and the 'lsqnonlin' routine to reach the global minimum are 27 and 378, respectively. Similarly, the number of iterations required for the proposed method and the 'lsqnonlin' routine to reach the global minimum are 13 and 18, respectively. Thus, explicitly computing the Jacobian and gradient as (12) and (14), respectively can make the optimization computationally more efficient.

VI. Conclusions

In this paper, a joint calibration and tomography (JCT) method based on a separable least squares approach is proposed. The proposed method models the tomography parameters and calibration parameters in the system model as linear and non-linear parameters. respectively. The proposed method uses the variable projection (VP) based constrained coupled least squares optimization. The imposition of constraints on the tomographic parameters improves the estimation accuracy of the ill-posed and under determined JCT problem. The constraints on the non-linear parameters restrict the proposed method from deviating far away from the initial guess, especially considering a good initial guess is available. In addition, this paper provides the approximated solutions for computing the Jacobian matrix and gradient vector which are required for solving the non-linear optimization problem. Simulated acoustic time of flight measurements are used to evaluate the proposed JCT method for reconstructing the temperature

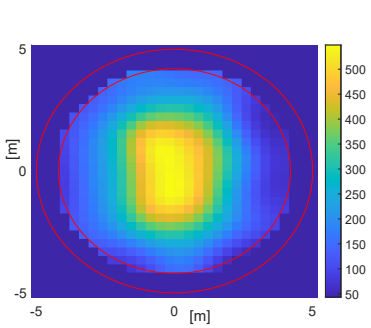

(a) Tomographic reconstruction using the JCT method with constraints only on the linear parameters.

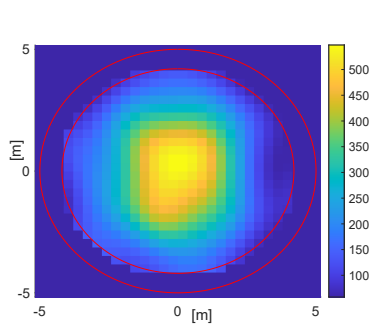

(b) Tomographic reconstruction using the JCT method with constraints on the linear and non-linear parameters.

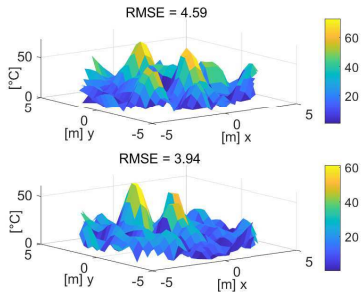

(c) The RMSE error of JCT method with constraints on linear parameters (upper) and constraints on the linear and non-linear parameters (lower).

Fig. 3: Reconstructed temperature distribution of the RoI using JCT based on VP method and the corresponding RMSE error.

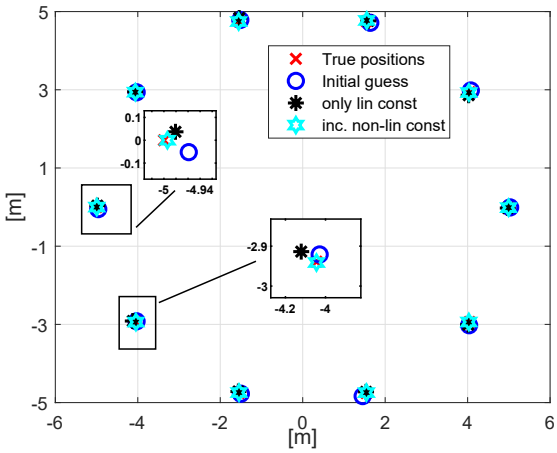

Fig. 4: Estimated positions of the transducers using JCT method with constraints on linear parameters and JCT method with constraints on linear and non-linear parameters.

distribution of a given region of interest and for calibrating the acoustic transducer positions. The proposed method achieves higher accuracy in both tomographic reconstruction and calibration compared to the method with constraints only on the linear parameters. The approximated Jacobian and gradient decrease the number of function evaluations and iterations required by the proposed method to converge to the global minimum compared to the finite difference approach used by non-linear optimization methods provided by Matlab.

ACKNOWLEDGMENTS

This work has been jointly supported by Infineon Technologies Austria AG, voestalpine Stahl GmbH and by Silicon Austria Labs (SAL), owned by the Republic of Austria, the Styrian Business Promotion Agency (SFG), the federal state of Carinthia, the Upper Austrian Research (UAR), and the Austrian Association for the Electric and Electronics Industry (FEEI).

The authors would like to thank Vera Ganglberger from voestalpine Stahl GmbH for her assistance in setting up the simulation setup.

REFERENCES

[1] J.A. Kleppe, “Engineering Applications of Acoustics”. *Artech House*, May, 1989.

[2] L. E. Larsen and J. H. Jacobi, “Medical Applications of Microwave Imaging”, *IEEE Press*, Jun. 1986.

[3] R. Parhizkar, A. Karbasi, S. Oh, and M. Vetterli, ”Calibration using Matrix Completion with Application to Ultrasound Tomography” in *IEEE Transactions on Signal Processing*, vol. 61, no. 20, 2013

[4] J. Yao and M. Takei, ”Application of Process Tomography to Multiphase Flow Measurement in Industrial and Biomedical Fields: A Review,” in *IEEE Sensors Journal*, vol. 17, no. 24, 2017.

[5] D. Zankl, S. Schuster, R. Feger, A. Stelzer, S. Scheiblhofer, C. M. Schmid, G. Ossberger, L. Stegfellner, G. Lengauer, C. Feilmayr, B. Lackner and T. Bürgler, ”BLASTDAR — A Large Radar Sensor Array System for Blast Furnace Burden Surface Imaging”, in *IEEE Sensors Journal*, vol. 15, no. 10, 2015.

[6] R. C. Aster, B. Borchers and C. H. Thurber, ”Parameter Estimation and Inverse Problems”, *Elsevier*, Oct. 2018.

[7] D. Ivan, R. Parhizkar, J. Ranieri and M. Vetterli, ”Euclidean Distance Matrices: Essential Theory, Algorithms, and Applications”, in *IEEE Signal Processing Magazine*, vol. 32, no. 6, 2015.

[8] A. Och, P. A. Hölzl, S. Schuster, J. O. Schrattenecker, P. F. Freidl, and S. Scheiblhofer, D. Zankl, V. Pathuri-Bhuvana and R. Weigel ”High-Resolution Millimeter-Wave Tomography System for Characterization of Low-Permittivity Materials”, in *IEEE MTT-S International Microwave Symposium*, 2020.

[9] D. Zankl, S. Schuster, R. Feger and A. Stelzer, ”Radar Array Self-Calibration and Imaging with Applications to Bulk Material Gauging”, in *proceedings of German Microwave Conference*, 2016.

[10] A. Cornelio, E. L. Piccolomini and J. G. Nagy,”Constrained Numerical Optimization Methods for Blind Deconvolution”, in *Springer Numerical Algorithms*, vol.65, no.1, 2014.

[11] G. H. Golub, and V. Pereyra, ”The Differentiation of Pseudo-Inverses and Nonlinear Least Squares Problems Whose Variables Separate”, in *SIAM Journal on Numerical Analysis*, vol. 10, no. 2, 1973.

[12] D. M. Sima, and S. V. Huffel, ”Separable Nonlinear Least Squares Fitting with Linear Bound Constraints and Its Application”, in *Elsevier Journal of Computational and Applied Mathematics*, vol. 203, no.1, 2007.

[13] C. Feilmayr, S. Schuster, V. Ganglberger, B. Lackner, D. Zankl and L. Stegfellner, ”Innovative Tools for Process Optimization – Burden Surface Scaning Via Beamforming Radar and Measurement of the Top Gas Temperature Distribution”, in *proceedings of 7th European Coke and Ironmaking Congress*, 2016.